Synthesis of ZnO thin film by chemical spray pyrolysis using its nano powder

Reem S. Khaleel[1], Mustafa Sh. Hashim[2, *], Samer Gh. Majeed[3]

[1,2]*Physics department, Education college, Mustansiriya University, Baghdad, Iraq*
[3] *The Central Service Laboratory, College of education Ibn Al Haitham,
Baghdad University, Baghdad, Iraq*

Corresponding author: mustmust@uomustansiriyah.edu.iq

Abstract

The deposition of metal oxides powder faces several problems, including poor adhesion to the bases deposited on them, the presence of many cracks, poor thickness control, and other disadvantages. The current study gives a new and simple idea to deposit thin films using two ZnO powders with nano and microparticle sizes on glass substrates. This was done by transforming the powders to Zinc acetate and then using chemical spray pyrolysis to deposit ZnO thin films. Scanning electron microscope (SEM) images showed that the prepared film from the nanopowder (ZnO_{Nano}) lost the independence of powder's nanoparticles and became a homogeneous film with nano projections. But the deposited one from the micro powder (ZnO_{Micro}) had both nanorods and nanoplates. The different shapes and sizes of ZnO particles in ZnO_{Micro} powder were disappeared after the Spray process. The two deposited films were homogeneous, crack-free and there were controllable thicknesses during the deposition. X-ray spectroscopy (EDS) was used to measure weights and atomic percentages of elements for the deposited films. The structures of the deposited films were approximately identical as the X-ray diffraction (XRD) technique showed. The optical properties of these two films were studied and their parameters were measured and calculated.

**Keywords**: Energy gap; powder; spray pyrolysis; zinc acetate; ZnO.

Researchers are encountering problems with the deposition of metal oxide powders using many techniques like electrophoretic deposition (Xiu *et al.*, 2008), atmospheric plasma spray (Barry *et al.*, 2013), Galvanic displacement deposition (Konstantin *et al.*, 2016). To overcome these problems many suggestions were discussed. The thermal treatment is a common procedure, but it can cause modifications in the film properties (Andressa *et al.*, 2015). The drop-casting technique was widely used to deposit nanopowder but it is not easy to get a homogeneous coating and not well controlled to get a desirable thickness (Norrman *et al.*, 2005). The spin coating technique is another method used to deposit nanopowder but unfortunately, it is having disadvantages. As the size of the sample rises, the high-speed spinning becomes hard. Generally, only 2% – 5% of material is dispensed onto the substrate, and 95%–98% of material is thrown off throughout the process (Bekir *et al.*, 2019). The dip-coating process is another technique utilized by a researcher to deposit nanopowder, but it has also a drawback. It is slow and masking is necessary because all components are submersible (Sarat *et al.*, 2018). On the other hand, spray pyrolysis has multiple

advantages over other techniques: it can be easily performed, substrates with complex geometries can be coated and relatively uniform and high-quality films can be deposited. The coatings of this technique are more durable than other techniques and wide precursor types could be used (Lado, 2012).

In this contribution, there is an attempt to deposit ZnO_{Nano} and ZnO_{Micro} powders on glass substrates using the spray pyrolysis technique after transforming these two powders to zinc acetate. There is also an investigation of the optical and structural properties of deposited films.

2. Experimental part

$ZnO_{Nanopowder}$ was produced using Rapid Breakdown Anodization (RBA) technique, the details of this method and the characterization of produced powder are reported in detail by the authors (Reem *et al.*, 2020). Zinc acetate powder was formed by immersing 1g ZnO_{Nano} inside 5ml acetic acid (Molarity: 60.05**)** as in the following equation.

$$ZnO + 2CH_3COOH \rightarrow Zn\,(CH_3CO_2)_2 + H_2O$$
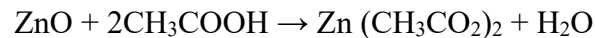
The produced salt has white color, and it was verified that the product was zinc acetate by dissolving it in water and this was done completely and immediately. 1g Zinc acetate was dissolved in 100ml distilled water and a clear precursor was obtained. During deposition, the substrate was put on a hot plate maintained at 350^0C. The distance between the glass nozzle and substrate was 28 cm. A carrier gas of chemical solution was the air with 2ml/min spraying rate. Commercial ZnO_{Micro} powder (PHWE, purity 99.999) was used to deposit ZnO films (sample1) on glass substrates. The same procedure was repeated for $ZnO_{Nanopowder}$ to deposit (sample2). The crystalline nature of the film's materials was tested by powders X-ray Diffractometer using Cu Kα radiation. XRD patterns were analyzed by indexing their peaks by XRD Powder Diffraction Files (PDF) type Ken Lagarec (version 1992-1996). UV-visible spectrophotometer type (CARY 100Conc) was utilized to record optical absorbance and transmittance in the (300-900nm) wavelength range. The compositions of used and produced materials were specified by Energy-dispersive X-ray spectroscopy EDS type (ARYA Electron Optic) with the following analysis conditions (Accelerating Voltage (kV):15, Beam Current (nA):10,000, Dead Layer (um) of detector: 0.1). The shapes and the sizes of particles were investigated by SEM type (TESCAN Mira-3 SEM).

3. Results and discussion

Structure properties

Figure 1 illustrates the XRD pattern of sample 1 and sample 2 films. For both films seven peaks belonging to the ZnO structure. The minor difference between the two patterns may be due to the variance in particle sizes of ZnO_{Nano} and ZnO_{Micro} powders. The peak data list for the two deposited films is shown in Table 1. The comparison between the two samples illustrates the relative shift in XRD patterns. The crystallite sizes of two films were calculated for dominant peak (002) using the

Scherrer equation, the value of this parameter is smaller for sample 1. Figure 2 illustrates SEM images of the ZnO_{Micro} powder and sample 1.
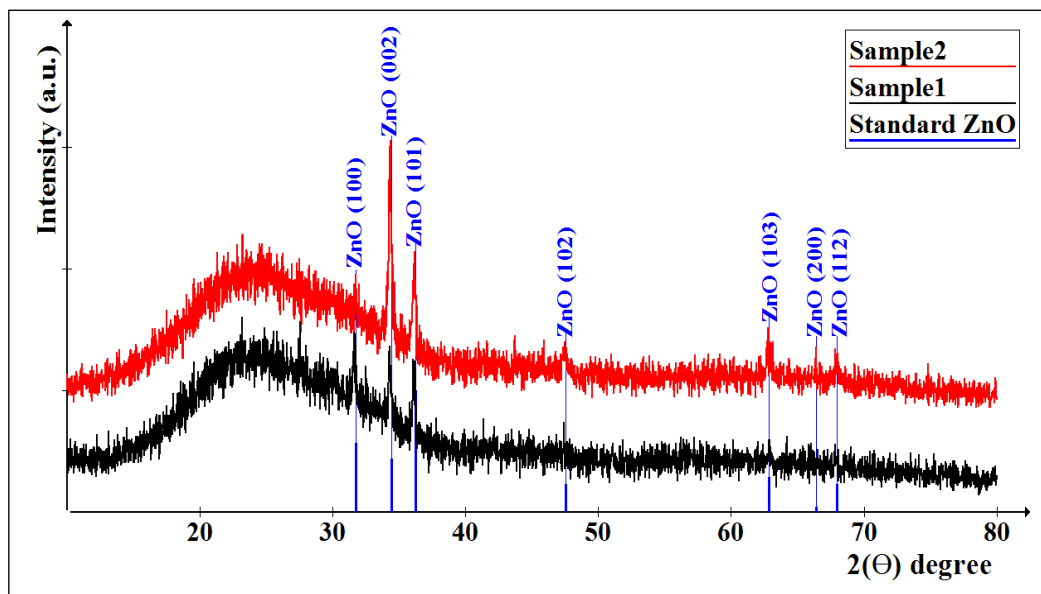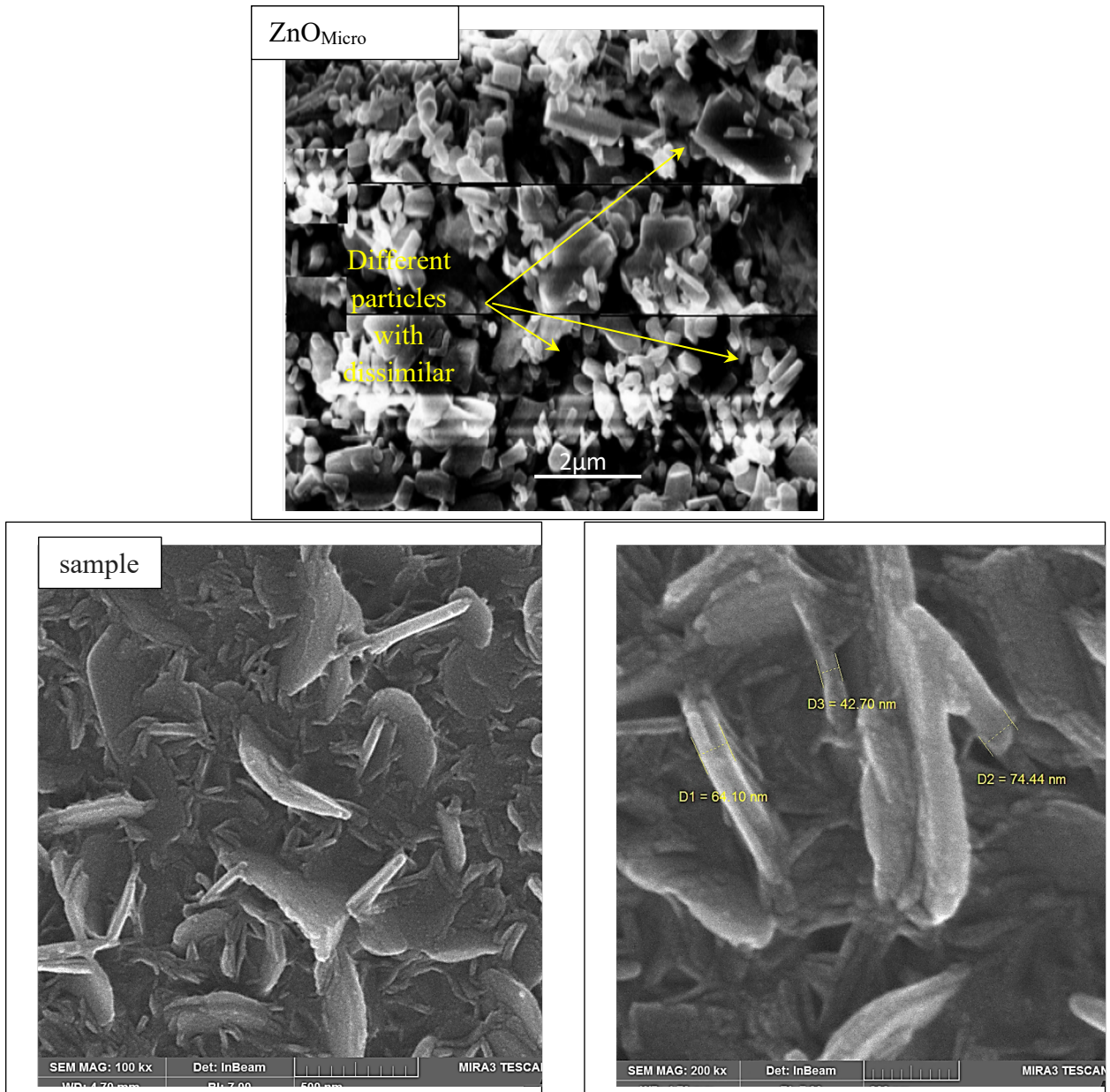

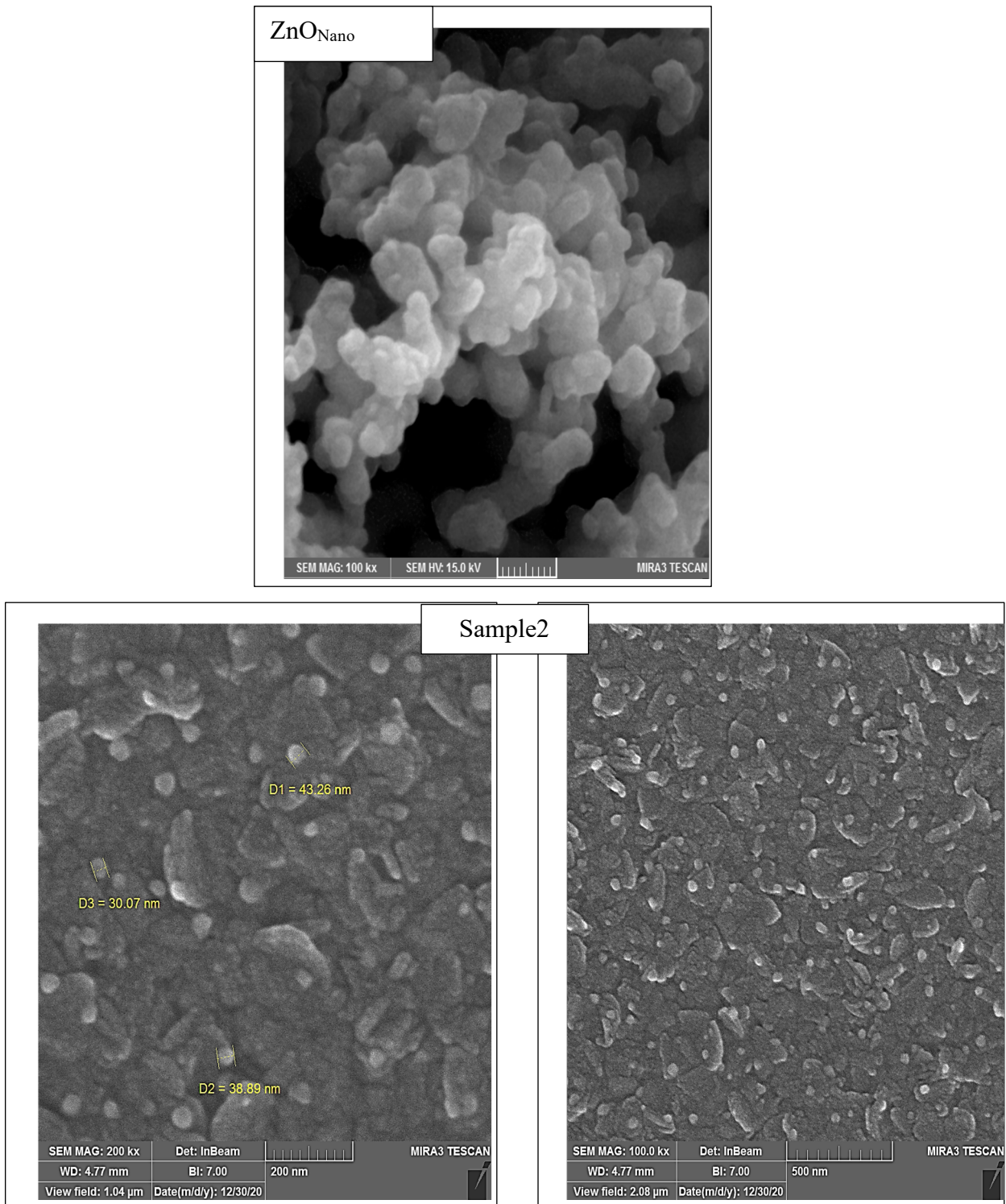**Fig. 1.** XRD patterns of the two deposited samples

Table 1. Peak data list

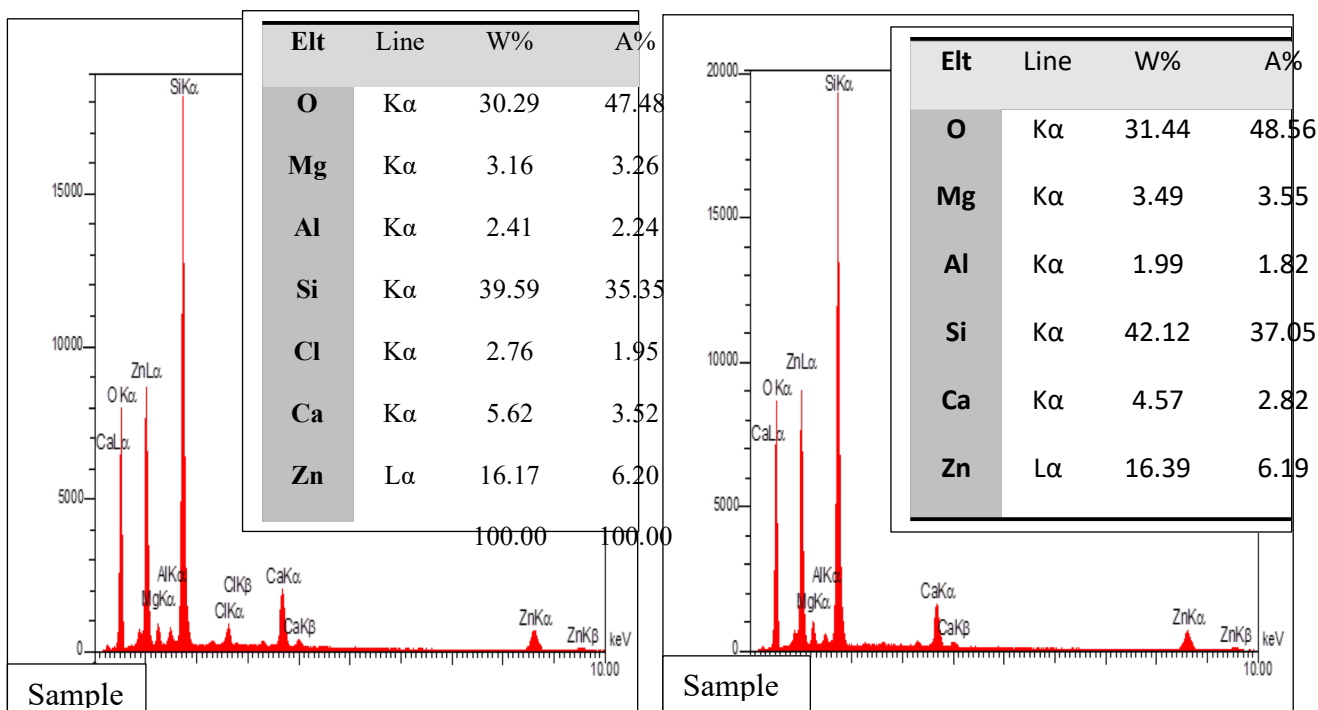| Film Type	Miller indices	2Theta (deg.)	FWHM (deg.)	Crystallite size(nm)
Sample1	(100)	31.6563	0.61	
Sample2		31.7562	0.19	
Sample1	(002)	34.3335	0.53	15.3
Sample2		34.3541	0.29	27.3
Sample1	(101)	36.1419	0.59	
Sample2		36.1519	0.27	

Fig. 2. SEM images of ZnO$_{Micro}$ powder and sample 1

These images display the transformation of sizes and shapes of ZnO$_{Micro}$ powder particles after conversion to dissolved zinc acetate and Spray process. The shapes of sample 1 particles were disoriented nanorods and nano-standing plates on a glass substrate. This result confirms that the current procedure can transform the powders into a thin film that has the same structure with improved properties.

Figure 3 depicts SEM images of ZnO$_{Nanopowder}$ and sample 2. After the deposition process, the produced film is crack-free, homogeneous, and has nano protrusions. EDS spectrum of sample 1 and sample 2 are presented in figure 4.

Fig.3. SEM images of ZnO$_{Nano}$ powder and sample 2.

Elt	Line	W%	A%
O	Kα	30.29	47.48
Mg	Kα	3.16	3.26
Al	Kα	2.41	2.24
Si	Kα	39.59	35.35
Cl	Kα	2.76	1.95
Ca	Kα	5.62	3.52
Zn	Lα	16.17	6.20
		100.00	100.00

| Elt	Line	W%	A%
O	Kα	31.44	48.56
Mg	Kα	3.49	3.55
Al	Kα	1.99	1.82
Si	Kα	42.12	37.05
Ca	Kα	4.57	2.82
Zn	Lα	16.39	6.19

Fig. 4. EDS spectrum of both films.

The elements O, Mg, Al, Si, Cl and Ca belong to the composition of substrate (Soda Lime Glass composition) (Mohd *et al.*, 2011). The remaining is made up of trace elements. W% and A% for both films were close together.

Optical properties

Transmittance% versus wavelength for the two deposited films is presented in Figure 5. This figure is used to calculate the thicknesses of deposited films by Swanepoel's Method (Shaaban *et al.*, 2012).

$$\text{Thickness}_{Sample1} = 442.5 \text{ nm}$$
$$\text{Thickness}_{Sample2} = 590.8 \text{ nm}$$
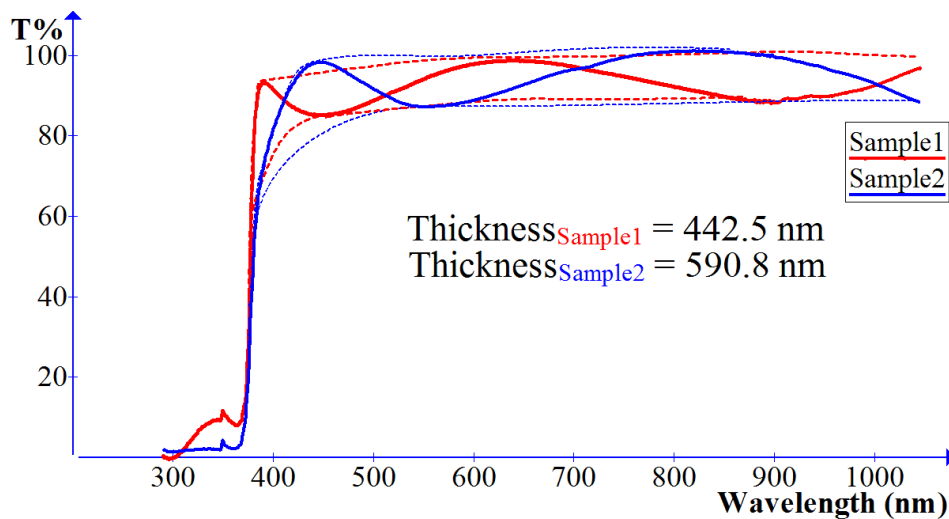
**Fig. 5.** Transmittance% versus wavelength for the samples

6

The thicknesses of samle1 and sample 2 were 442.5 nm and 590.8 respectively. Greater than 400 nm; the transmittance% of two films is more than 80%. This optical property can be exploited to use these films as a window in solar cell applications (Norbert *et al.*, 2005).

The absorbance of deposited films against wavelengths is depicted in Figure 6(A). Near the fundamental absorption edge, the two ZnO films show a very sharp absorption edge. The observed peaks at 361 nm and 353 nm for the two samples are comparable to that obtained by (Neli *et al.*, 2012) who synthesized nanospheres and nanorods ZnO by Chemical spray pyrolysis technique.

There is a blue shift of the maximum absorption peak for sample 2 compare with that of sample1. This can be attributed to the difference in particle sizes for both samples (Elmira *et al.*, 2016) as SEM images confirm.

Figure 6(B) illustrates the absorbance of the dissolved Zinc acetates in water produced by using ZnO_{Nano} and ZnO_{Micro} powders. The fundamental absorption edges for both solutions occurred at the UV region where they were invisible regions for deposited films. The peak at a wavelength of approximately 210 nm was observed by (Teterycz *et al.*, 2013) for ethylene glycol solution containing zinc acetate. In general, the absorbance of zinc acetate solution of sample 2 is greater than that for sample 1, this may be due to the particles' sizes of ZnO_{Nano}.

One of the most important optical constants is the energy gap (Eg); Figure 7 shows the calculation of Eg for the two films by using tauc formulas.
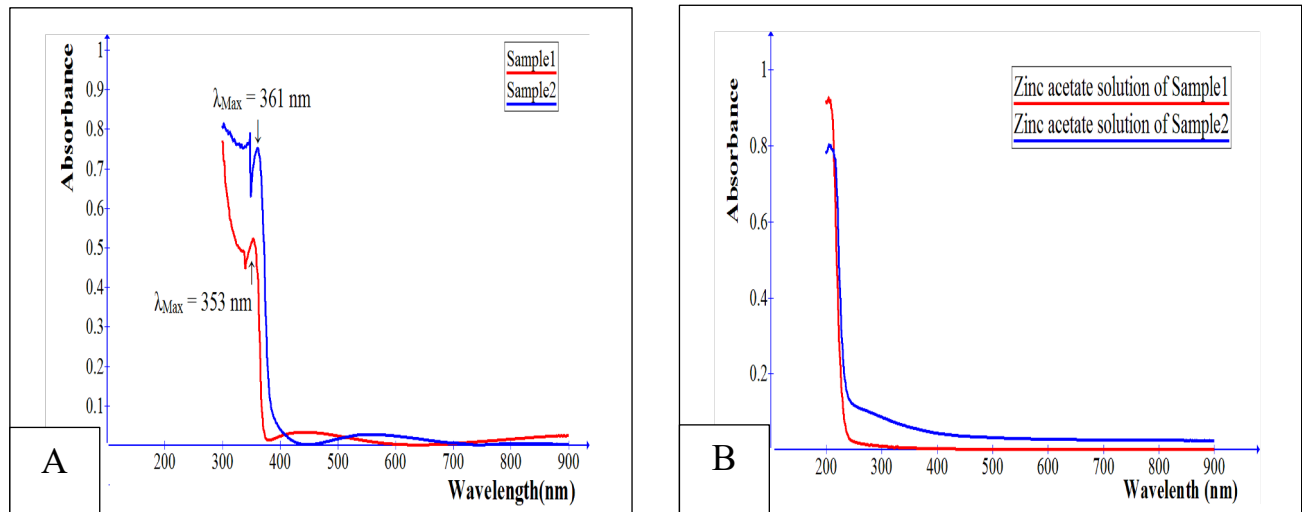
Fig. 6. Absorbance against wavelength for: (A)deposited films, (B) Zinc acetate solutions.
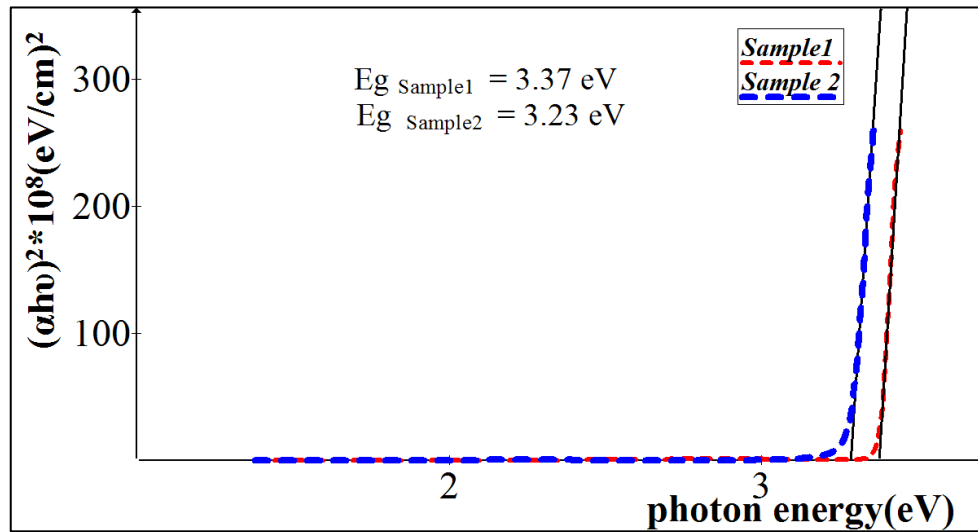
Fig. 7. Calculation of energy gaps for the two films

The values of Eg for the two films are 3.37 and 3.23 eV for sample 1 and sample 2 respectively. The value of Eg $_{sample1}$ film equals exactly that of Bulk ZnO material in agreement with that obtained by (Sanjeev *et al.*, 2015). For Eg $_{sample2,}$ is less than that of bulk ZnO compatible with that obtained by (Bindu *et al.*, 2017). The extent of non-stoichiometry of the deposited layers may be responsible for the reduction of Eg $_{sample2}$ (Nehru *et al.*, 2018). The relatively large value of Eg $_{sample1}$ may be due to the presence of high disorderedness compare with that of sample 2, see XRD patterns. (Kumar *et al.*, 2011) deposited amorphous ZnO film using physical vapor condensation method, Eg of this film was 3.75 eV, they attributed this result to the irregularity in their sample.

(Norlida *et al.*, 2015) concluded that the bandgap widening and narrowing in materials are very complex processes depending on whether they are micron or nano-sized crystallites and for nano ZnO material, the Eg widening can be mainly attributed to the larger downward shift of the valence band mechanisms.

The energy width of the tail of the localized state (E$_e$) in the normally forbidden bandgap for the two films is calculated as illustrated in Figure 8. The values of Ee are 0.036 and 0.056 eV for sample1 and sample 2 respectively.

Some causes perhaps affect Ee in a semiconductor, including structural disorder, carrier–phonon interaction and carrier–impurity (Byunggu *et al.*, 2017). Thus, the increased number of defects during deposition process of sample 2 film may be responsible for its relatively larger Ee value.
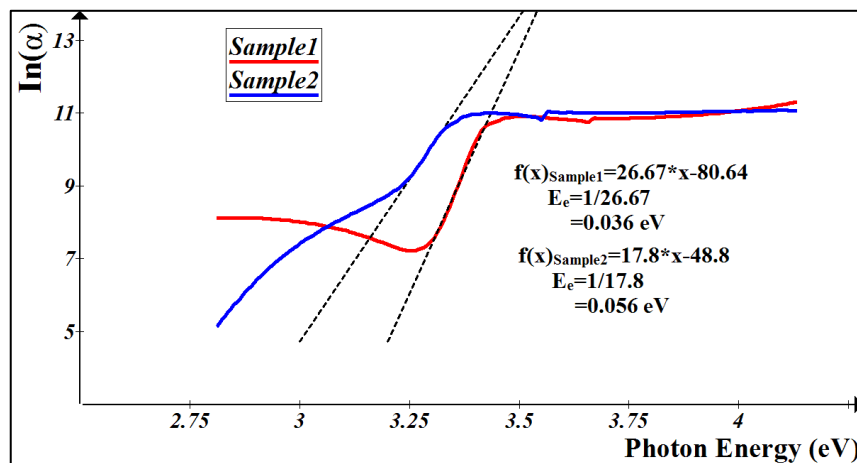
Fig. 8. Ubarch tail energy plot for the synthesized films.

Interpretation of the difference in the surface topographies

One of the possible causes that explain the difference in the surface topographies between the two samples is the difference in the properties of the droplets generated from each dissolved powder.

Because of the smaller size of the nanoparticles compared to that of the microparticles, the occupied volume by the nanoparticles of nano Zinc acetate differs from that occupied by the same material at the microscopic size. (Khammar *et al*., 2016) reported two points: (i) droplets of the same component but of different initial droplet volume or size have different evaporation lifetimes. (ii) If the droplets reaching the substrate have less solvent and more salt, a less porous or more compact film is formed.

So, it can be concluded that the initial different droplets of the two dissolved powders produced dissimilar ZnO films.

4. Conclusions

The process of converting zinc oxide powder into thin films by the method presented with this work has proven high efficiency by obtaining films that have features that the original powder does not possess. The two deposited films were homogeneous, crack-free and had different morphology. The difference with the primary powder produced ZnO films with different optical properties.

References

Andressa C. Schneid, Marcelo B. Pereira, Flavio Horowitz, Raquel S. Mauler, Carla R. Matte, Manuela P. Klein, Plinho F. Hertz, Tania M. H. Costa, Eliana W. de Menezes & Edilson V. Benvenutti (2015). Silver Nanoparticle Thin Films Deposited on Glass Surface Using an Ionic Silsesquioxane as Stabilizer and as Crosslinking Agent. J. Braz. Chem. Soc., 26 **(5)** 1004-1012.

Bekir S.Yilbas & Abdullah Al-Sharafi Haider Ali (2019). Self-Cleaning of Surfaces and Water Droplet Mobility, springer Pp 45-98.

Byunggu Kim & Jae-Young Leem (2017). Effects of Doping Concentration on the Structural and Optical Properties of Spin-Coated In-doped ZnO Thin Films Grown on Thermally Oxidized ZnO Film/ZnO Buffer Layer/Mica Substrate, (Korean J. Met. Mater.) 55**(1)**, pp.67-71.

E.R. Shaaban, I.S. Yahia & E.G. El-Metwally (2012). Validity of Swanepoel's method for calculating the optical constants of thick films, Acta physica Polonica A, 121.

Elmira Solati & Davoud Dorranian (2016). Effect of temperature on the characteristics of ZnO nanoparticles produced by laser ablation in water, Bull. Mater. Sci., 39 **(7)**, pp. 1677–1684.

Helena Teterycz, Olga Rac, Patrycja Suchorska –Wozniak & Dominika Oles (2013). The Formation Mechanism of Colloidal Spheres of ZnO in Ethylene Glycol, Digest Journal of Nanomaterials and Biostructures, 8**(3)**, pp. 115 7 – 1167.

J. N. Barry, B. Twomey, A. Cowley, L. O'Neill, P. J. McNally & D. P. Dowling (2013). Evaluation and comparison of hydroxyapatite coatings deposited using both thermal and non-thermal techniques. Surface and Coatings Technology, 226: 82-91.

K. Norrman, A. Ghanbari-Siahkali& N. B. Larsen (2005). Studies of spin-coated polymer films, Annu. Rep. Prog. Chem. Sect. C 101: 174–201.

Konstantin I. Popov, Stojan S. Djokic, Nebojsˇa D. Nikolic & Vladimir D. (2016). Jovic, Morphology of Electrochemically and Chemically Deposited Metals, Springer. **Pp 344**.

L. C. Nehru, M. Umadevi, C. Sanjeeviraja (2012). Studies on Structural, Optical and Electrical Properties of ZnO Thin Films Prepared by the Spray Pyrolysis Method, International Journal of Materials Engineering, 2(1): 12-17.

Lado F. (2012). Topography Simulation of Novel Processing Techniques, Ph.D. thesis, Sarajevo, Jugoslawien.

M. Khammar, S. Guitouni, N. Attaf, M.S. Aida (2016). Droplet Lifetime under Spray Pyrolysis Deposition Conditions, International Journal of ChemTech Research.9 **(08)** pp 374 -381.

Mohd S. Ab Karim, Ahmed Aly Diaa M. Sarhan & Mohd H. Abd Shukor (2011). Experimental Study on Minimizing Edge Chipping in Glass Milling Operation Using an Internal CBN Grinding Tool, Materials and Manufacturing Processes, 26: 969 – 976.

Neli Mintcheva, Ali A. Aljulaih, Wilfried Wunderlich, Sergei A. Kulinich & Satoru Iwamori (2018). Laser-Ablated ZnO Nanoparticles and Their Photocatalytic Activity toward Organic Pollutants. Materials, 11: 1127.

Norbert H. Nicke &Evgenii Terukov (2004). Zinc Oxide - A Material for Micro- and Optoelectronic Applications, springer pp 197-209.

Norlida Kamarulzaman, Muhd F. Kasim & Roshidah Rusdi (2015). Bandgap Narrowing and Widening of ZnO Nanostructures and Doped Materials. Nanoscale Research Letters, 10: pp.346.

P. Bindua, and S. Thomas (2017). Optical Properties of ZnO Nanoparticles Synthesized from a Polysaccharide and $ZnCl_2$, ACTA PHYSICA POLONICA A, 131.

Ravi K. Kumer, M. Husain & Zishan H. Khan (2011). Optical Studies on Amorphous ZnO Film, Digest Journal of Nanomaterials and Biostructures, 6 **(3)** pp. 1317-1323.

Reem S. Khaleel & Mustafa Sh. Hashim (2020). Fabrication of ZnO sensor to measure pressure, humidity and sense vapors at room temperature using the rapid breakdown anodization method. Kuwait J. Sci. 47 **(1)**: 42-49.

Sandeep Sanjeev & Dhananjaya Kekuda (2015). Effect of Annealing Temperature on the Structural and Optical Properties of Zinc Oxide (ZnO) Thin Films Prepared by Spin Coating Process, IOP Conf. Series: Materials Science and Engineering 73, 012149.

Sarat K. Sahoo, Balamurugan M. & Narendiran S. (2018). Basic to Advanced Concepts and Implementation, Academic press. Pp 1-24.

Xiu F. Xiao, Rong F. Liu & Xiao L. Tang (2008). Electrophoretic deposition of silicon substituted hydroxyapatite coatings from n-butanol–chloroform mixture. Journal of Materials Science: Materials in Medicine, 19: 175–182.